MULTIBASELINE POLARIMETRIC SAR INTERFEROMETRY FOREST HEIGHT INVERSION APPROACHES

SeungKuk Lee[(2)(1)], Florian Kugler[(1)], Kostas Papathanassiou[(1)] , Irena Hajnsek[(2)(1)]

[(1)]German Aerospace Center (DLR), Microwave and Radar Institute (HR), Germany, Email:seungkuk.lee@dlr.de
[(2)]ETH Zurich, Institute of Environmental Engineering, Switzerland

ABSTRACT

Polarimetric SAR interferometry (Pol-InSAR) is a radar remote sensing technique that is sensitive to the vertical distribution of scattering processes in volumes. The Random Volume over Ground (RVoG) model is a powerful tool used to invert forest height from Pol-InSAR data. But Pol-InSAR inversion performance depends critically on uncompensated decorrelation contributions (i.e. temporal decorrelation in repeat pass system) and the height sensitivity of the effective baseline, represented by the vertical wavenumber κ_z . To overcome these constraints a multibaseline Pol-InSAR inversion approach could be an effective solution. In this paper, different approaches for combining multibaseline Pol-InSAR inversion results are proposed and discussed. Multibaseline Pol-InSAR data acquired by DLR's E-SAR system over the Traunstein forest during the TempoSAR 2008 campaign are used.

1. INTRODUCTION

The coherent combination of both interferometric and polarimetric observations by means of polarimetric SAR interferometry (Pol-InSAR) allows the identification and separation of the different scattering contributions within the resolution cell and is therefore sensitive to the vertical structure of volume scatterer [1][2][3]. In the last years, quantitative model based estimation of forest parameters - based on single frequency fully polarimetric single-baseline configuration - has been developed and demonstrated over a variety of test sites [1][2][4][5][6].

The key observable used in Pol-InSAR application is the complex interferometric coherence $\tilde{\gamma}$ (including both the interferometric correlation coefficient and the interferometric phase) measured at different polarizations. The interferometric coherence depends on instrument and acquisition parameters as well as on dielectric and structural parameters of scatterers. After the calibration of system-induced decorrelation and compensation of spectral decorrelation, the estimated interferometric coherence can be decomposed into volume decorrelation $\tilde{\gamma}_{Vol}$ used mainly in Pol-InSAR inversion and other non-volumetric decorrelation contributions. In general uncompensated non-volumetric decorrelation contributions reduce the successful implementation of Pol-InSAR parameter inversion. Among these non-volumetric decorrelation contributions, the most critical factor for Pol-InSAR inversion is temporal decorrelation caused by changes of scatterers within the scene in terms of a conventional airborne/spaceborne repeat-pass system.

In addition to temporal decorrelation, Pol-InSAR height inversion performance is also affected by the vertical wavenumber κ_z . The vertical wavenumber κ_z is the key parameter for Pol-InSAR inversion. It scales the height sensitivity and determines the available height range possible to invert. Therefore, an inappropriate vertical wavenumber (e.g. too large or too small κ_z) for a certain forest height leads to ill-conditioned height inversion problems resulting in under-/overestimation of forest height.

To counter these constraints and to improve the quality of forest parameter inversion multibaseline Pol-InSAR inversion approach has been proposed and developed [4]. There are two different ways to do this: The one is a "coherent" combination which means to get one height value from all used baselines on the level of complex coherence estimates. In this case relative and absolute baseline to baseline phase calibrations are required [7]. The other is to estimate individually single baseline Pol-InSAR inversion heights and then to combine them, so called the "incoherent" approach. It becomes therefore a key issue how several Pol-InSAR acquisitions can be effectively combined.

In this study, two different incoherent methods are investigated: The first one is the combination/selection of individual inversion heights by using the eccentricity of the coherence boundary [11]. The shape and size of the coherence boundary are determined by uncompensated decorrelation effects, and besides, the differences in the ground contribution between polarizations. The second criterion used to combine multiple baselines is the conventional interferometric height accuracy defined by the standard deviation of the interferometric phase [8] and the vertical wavenumber κ_z . The increase of the standard deviation of the interferometric phase with decreasing coherence caused by decorrelation contributions reduces the quality of the height accuracy and the successful forest height inversion.

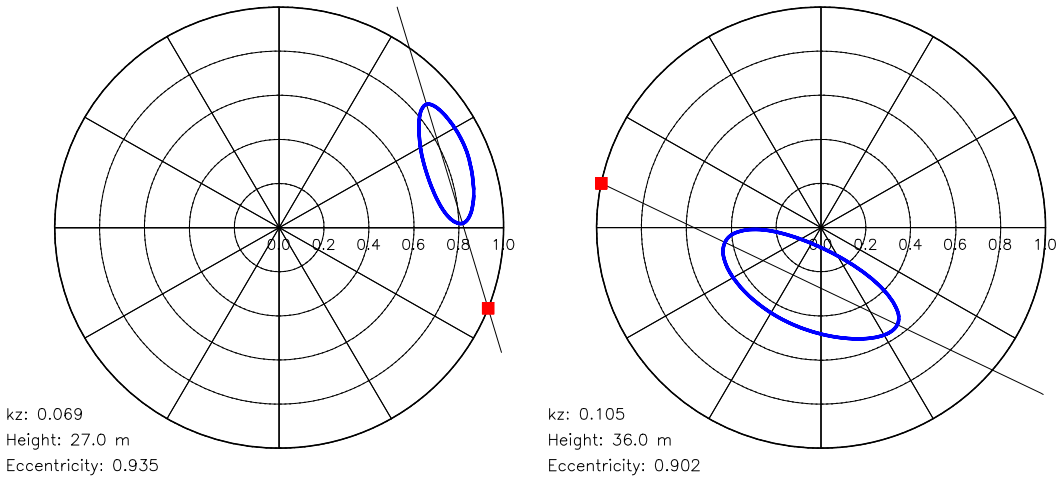

Figure 1. Coherence boundaries plotted in the unit circle for one pixel observed by two different baselines (κ_z =0.069 and 0.105). Blue ellipse: coherence boundary, Red point: ground phase.

2. POL-INSAR INVERSION TECHNIQUE

2.1. Single Baseline Pol-InSAR Inversion

The interferometric coherence $\tilde{\gamma}$ is estimated by the normalized cross correlation of the two co-registrated SAR images obtained from slightly different interferometric acquisitions s_1 and s_2 at different polarizations as indicated by the unitary vector $\vec{w}$ [1][2]

$$\tilde{\gamma}(\vec{w}) := \frac{< s_1(\vec{w}) s_2^*(\vec{w}) >}{\sqrt{< s_1(\vec{w}) s_1^*(\vec{w}) >< s_2(\vec{w}) s_2^*(\vec{w}) >}}. \qquad (1)$$

This interferometric coherence consists of different decorrelation contributions.

$$\tilde{\gamma} := \tilde{\gamma}_{Temp}\, \gamma_{SNR}\, \tilde{\gamma}_{Vol} \qquad (2)$$

Temporal decorrelation $\tilde{\gamma}_{Temp}$ depends on forest structure, the temporal stability of the scatterers and the temporal baseline of the interferometric acquisition. Noise decorrelation γ_{SNR} is induced by the additive white noise contribution on the received signal [9][10]. Volume decorrelation $\tilde{\gamma}_{Vol}$ is the decorrelation caused by the different projection of the vertical component of the scatterer into two images $s_1(\vec{w})$ and $s_2(\vec{w})$. $\tilde{\gamma}_{Vol}$ is directly linked to the vertical distribution of scatterers $F(z)$ through a (normalized) Fourier transformation relationship [15]:

$$\tilde{\gamma}_{V0} = \exp(i\kappa_z z_0) \frac{\int_0^{h_v} \exp(i\kappa_z z') \exp\left(\frac{2\,\sigma\, z'}{\cos\theta_0}\right) dz'}{\int_0^{h_v} \exp\left(\frac{2\,\sigma\, z'}{\cos\theta_0}\right) dz'} \qquad (3)$$

where h_v is the height of the volume and κ_z the effective vertical wavenumber. θ_0 is the incidence angle and σ a mean extinction coefficient.

The vegetation is modeled as a volume layer of certain thickness containing randomly oriented particles with given backscattering amplitude per volume unit. The random volume is located over an impenetrable ground scatterer represented by its own backscattering amplitude. A widely and successfully used model for $F(z)$ is the so-called Random Volume over Ground (RVoG) model, composed of a vegetation layer and a ground component comprising all scattering components with a phase center located on the ground.

$$\tilde{\gamma}_{Vol} = \exp(i\kappa_z z_0) \frac{\tilde{\gamma}_{V0} + m}{1 + m} \qquad (4)$$

where m is the ground to volume ratio $m = m_G / (m_V I_0)$ and accounts for the amount of ground scattering within the signal.

In case of a single baseline Quad-pol interferometric acquisition three measured complex coherences [$\tilde{\gamma}(\vec{w}_1)$ $\tilde{\gamma}(\vec{w}_2)$ $\tilde{\gamma}(\vec{w}_3)$] each for any independent polarization channel [3] are available to estimate six real

unknowns ($h_v, \sigma, m_{1-3}, \phi_0$). Assuming no response from the ground in one polarization channel (i.e. m_3=0), the inversion problem has a unique solution and is balanced with five real unknowns and three measured complex coherences ($h_v, \sigma, m_{1-2}, \phi_0$)

$$\min_{h_v,\sigma,m_i,\phi_0} \left\| \begin{bmatrix} \tilde{\gamma}(\vec{w}_1) \\ \tilde{\gamma}(\vec{w}_2) \\ \tilde{\gamma}(\vec{w}_3) \end{bmatrix} - \begin{bmatrix} \tilde{\gamma}_V(h_v,\sigma,m_1) \\ \tilde{\gamma}_V(h_v,\sigma,m_2) \\ \tilde{\gamma}_{V0} e^{i\phi_0} \end{bmatrix} \right\| \qquad (5)$$

However, this model does not account for decorrelation effects introduced by dynamic changes within the scene occurring in the time between the two acquisitions.

2.2. **The Coherence Region**

In Pol-InSAR inversion it is important to determine the maximum coherence change with polarization since it indicates the information about the vertical distribution of the scattering mechanisms. To visualize this, a geometrical interpretation, the so called "Coherence Region (CR)" has been used [11]. For a given polarimetric interferometric matrix there will be some sub-region of the unit circle that encloses all possible values of coherence (for all states of $\vec{w}$, see Eq. (1)) [13]. This is called the Coherence Region (CR) of the polarimetric interferometric matrix. In general the shape and size of the region are determined by the nature of the scattering processes and the interferometric geometry (and the number of looks L_{Int}). The boundary of the coherence region can be computed numerically for the constrained case ($\vec{w}_1 = \vec{w}_2$) using the eigenvalue equation derived in [11][12][13]

$$\tilde{\gamma}(\vec{w},\phi) = \frac{\vec{w}^{*T}\left[\tilde{\Omega}\right]\vec{w}}{\vec{w}^{*T}\left[T\right]\vec{w}} \Rightarrow \left[T\right]^{-1}\left[\tilde{\Omega}\right]\vec{w} = \lambda\vec{w} \qquad (6)$$

where $\tilde{\Omega} = (\Omega_{12}e^{i\phi} + \Omega_{12}^{*T}e^{-i\phi})/2$ and $T = (T_{11} + T_{22})/2$.
For each rotation angle ϕ the eigenvalue equation (Eq. (6)) yields the maximum and minimum eigenvalues and eigenvectors which can be used to estimate two coherences on the boundary of the coherence region. By varying ϕ within the interval $[0,\pi)$ the whole boundary of the coherence region can be reconstructed [13] as shown in *Figure 1*.

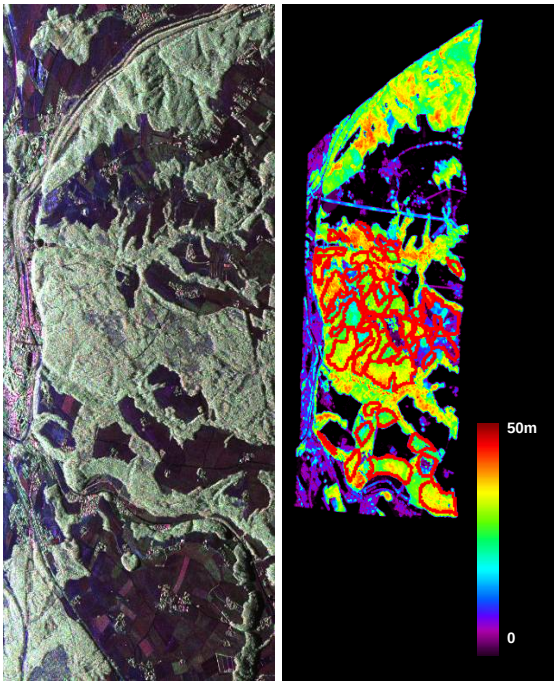

Figure 2. Traunstein test site. Left: Radar image of the Pauli components, red: HH-VV, blue: HH+VV, green: HV, Right: Lidar H100 image overlaid with validation stands scaled from 0 m to 50 m.

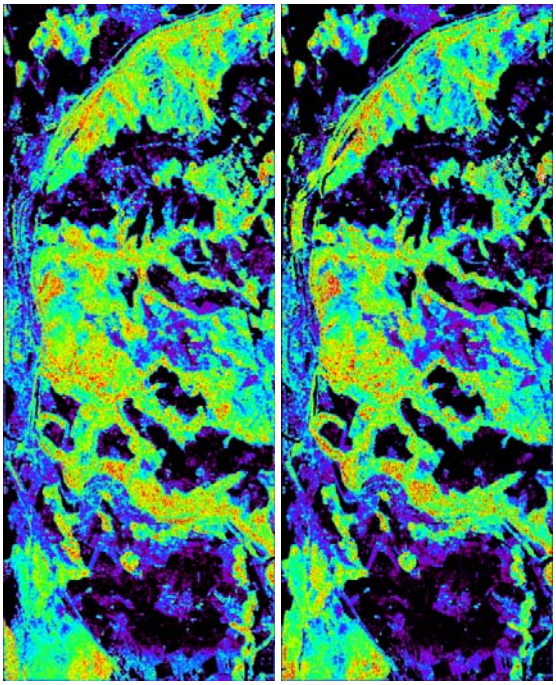

Figure 3. Multibaseline Pol-InSAR forest height maps scaled from 0 m to 50 m (see the color table in Figure 2). Left: the eccentricity method, Right: the height accuracy method.

3. THE MULTIBASELINE POL-INSAR COMBINATION CRITERION

In this section two different incoherent methods for baseline combination are discussed. One possibility is to combine all obtained height estimates weighted by individual criterions which reduce the variation of the height estimates from the different baselines. However, when a bias induced for example by temporal decorrelation is not excluded from the inversion results, the error of the weighted mean height increases. For this reason, instead of linear combination, the best height estimate will be selected from all obtained inversion heights by using a certain criterion.

3.1. The Eccentricity of the Coherence Boundary

The coherence region of the polarimetric interferometric matrix is a straight line segment [3], where the length of the line depends on acquisition parameters such as the vertical wavenumber and on scattering parameters such as the volume height, the extinction level of the vegetation layer and more important the range of the ground-to-volume scattering ratio with polarization. Longer line segments correspond primarily to a wide ground-to-volume scattering ratio range. This improves the conditioning of the inversion and increases the estimation accuracy.

However, estimation uncertainties due to the non-unit coherence level as well as deviations from the underlying model assumptions (RVoG) lead to a more ellipse-like shaped coherence region rather than a straight line. Thus, (see *Figure 1*) the shape of the ellipse (coherence region) can be used as an indicator for the estimation accuracy for each individual case: An elongated ellipse can be associated to better inversion performance than a circular one [4].

The eccentricity of coherence boundary can be used as criterion when combining results obtained from different spatial baselines:

$$Eccentricity\ (e) = \sqrt{1-(b/a)^2} \tag{7}$$

where a is the major axis and b is the minor axis of the ellipse. In *Figure 1* an example of two coherence boundaries obtained for the same forest stand from two different spatial baselines is shown. The eccentricities of the two ellipses are 0.935 and 0.902 indicating that in this particular case the height estimates obtained from the smaller baseline (κ_z = 0.069) are more reliable than the ones obtained from the larger baseline (κ_z = 0.105).

When more than two Pol-InSAR measurements are available, the inversion height for the baseline corresponding to the largest eccentricity will be selected

$$\max_{h_v,\sigma,m,\phi_0} \begin{Vmatrix} e^1(\kappa_z^1,\ \Omega_{12}^1,\ T^1) \\ e^2(\kappa_z^2,\ \Omega_{12}^2,\ T^2) \\ \vdots \\ e^N(\kappa_z^N,\ \Omega_{12}^N,\ T^N) \end{Vmatrix} \tag{8}$$

where N is the number of available baselines for each pixel.

3.2. Height Accuracy

A second criterion used to select the "best" estimate from multibaseline inversion results is defined by the conventional interferometric height accuracy defined by the standard deviation of the interferometric phase ϕ_{Int} [8] and the vertical wavenumber κ_z

$$H_{accuracy} = -\frac{1}{\kappa_z}\phi_{Int} \tag{9}$$

$$\text{with}\quad \phi_{Int} = \sqrt{\frac{1-\gamma^2}{2\ L_{Int}\gamma^2}} \tag{10}$$

γ is the interferometric coherence and L_{Int} the number of looks used for the estimation of γ [10]. When the amplitude of γ is reduced by non-volumetric decorrelation contributions (i.e. temporal decorrelation), the standard deviation ϕ_{Int} of the interferometric coherence increases and the height accuracy becomes consequently deteriorated. It means the lower height accuracy indicates a more reliable inversion result. When multibaseline forest inversion estimates are available, the one that corresponds to the minimum height accuracy is selected

$$\min_{h_v,\sigma,m,\phi_0} \begin{Vmatrix} H_{accuracy}^1(\kappa_z^1,\ \gamma^1,\ L_{\text{int}}) \\ H_{accuracy}^2(\kappa_z^2,\ \gamma^2,\ L_{\text{int}}) \\ \vdots \\ H_{accuracy}^N(\kappa_z^N,\ \gamma^N,\ L_{\text{int}}) \end{Vmatrix} \tag{11}$$

where N is the number of baselines.

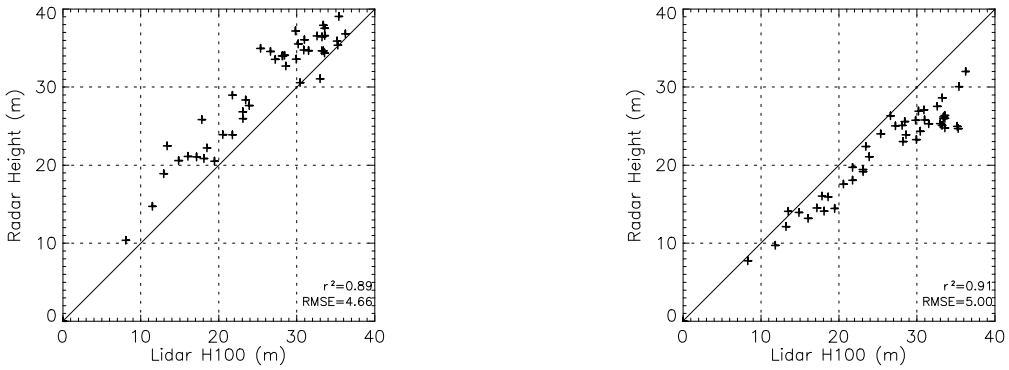

Figure 4. Validation plots multibaseline inversion: Pol-InSAR height estimates from TempoSAR campaign 2008 vs. Lidar h100 reference height; Left: Mean height, Right: Minimum height.

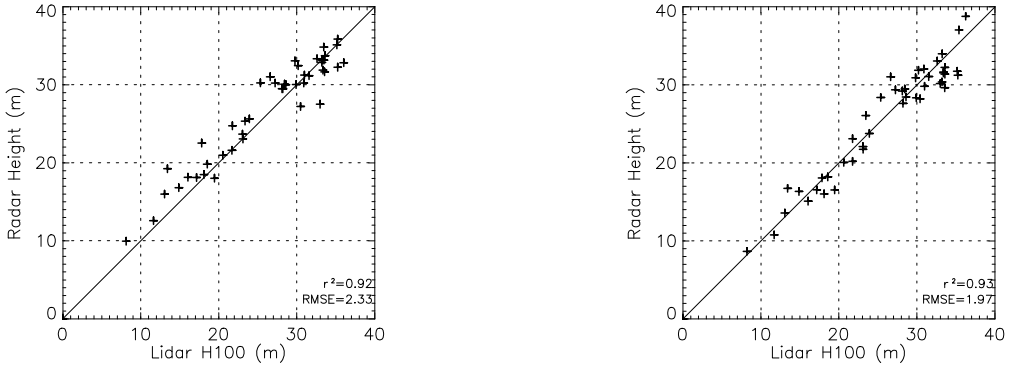

Figure 5. Validation plots multibaseline inversion: Pol-InSAR height estimates from TempoSAR campaign 2008 vs. Lidar h100 reference height; Left: the eccentricity method, Right: the height accuracy method.

4. TEST SITE AND DATA SET

The Traunstein test site (see *Figure 2*) is located in the southeast of Germany (47°52' north, 12°39' east), next to the city Traunstein to the east. Topography varies from 530 – 650m amsl, with only few steep slopes. The climatic conditions with a mean annual temperature of 7.8°C and precipitation of more than 1600 mm/year favor mixed mountainous forests, dominated by Norway spruce (Picea abies), beech (Fagus sylvatica) and fir (Abies alba). On a global scale this forest type is part of the temperate forest zone. It is a managed forest composed of even-aged stands which cover forest heights from 10 m to 40 m. Mean biomass level is on the order of 210 t/ha while some old forest stands can reach biomass levels up to 500 t/ha.

The TempoSAR 2008 campaign was performed in June 2008. DLR's E-SAR system in a repeat pass mode collected fully polarimetric and interferometric SAR data at L-band over the Traunstein test site six times within 13 days. A radar image of the Pauli components is shown in *Figure 2* on the left. The data set obtained on the 13th of June 2008 was selected for this study. The selected spatial baselines are -15, -5, 0, 5, 10 m and the temporal baseline is between 10 and 50 minutes. During the TempoSAR 2008 campaign Lidar reference data were acquired for validation of the Pol-InSAR height estimates at L-band. The Lidar forest height map is displayed in *Figure 2* on the right.

5. RESULTS AND DISCUSSION

After compensating for systematic decorrelation contributions and masking the non-valid areas by using a coherence mask (γ <0.4) and a κ_z mask (κ_z <0.05 or κ_z >0.15), forest heights for the valid area (unmasked) of each baseline are estimated. In order to improve forest height inversion results single baseline inversion

heights are then incoherently combined by means of the eccentricity of coherence boundary method (Eq. (8)) and the height accuracy method (Eq. (11)). Multibaseline forest height maps are shown in *Figure 3*.

Before using the two methods suggested in section 3, two straightforward ways of combining height estimates from different baselines are discussed: The first one is the mean method, which simply takes an average of all available measurements. While eccentricity and height accuracy methods try to filter unfavorable decorrelated measurements, the mean method includes all measurements for a combined height estimate. Some of the measurements are strongly affected by non-volumetric decorrelation (i.e. temporal decorrelation) introduce a bias (overestimation). This is confirmed by the validation plot in *Figure 4* on the left. Here forest heights are clearly overestimated with a RMSE of 4.66m.

The second one is the minimum method that takes the lowest height value among available inversion results. It is assumed that all height estimates larger than the minimum height are affected by undesirable decorrelation processes such as temporal decorrelation. The validation result for the minimum method can be found in *Figure 4* on the right. Up to a forest height of 15 m the minimum method has convincing results. Beyond 15 m a clear underestimation of forest heights can be observed, that becomes more critical with increasing forest height, resulting in a RMSE of 5 m. The underestimation for large forest stands can be explained by means of the used vertical wavenumber κ_z mask. For example, an upper κ_z boundary of 0.12 does not cover tree heights larger than 35 m. Nevertheless tree heights larger than 35 m appear in particular in the taller stands of the test site. In this case taking the minimum inversion result corresponds to selecting a height estimate from an insensitive (saturated) baseline that causes underestimation in the relatively tall forest stands.

The validation plots for the eccentricity method (Eq. (9)) and the height accuracy method (Eq. (11)) discussed in section 3 are displayed in *Figure 5*. By using reliable criterions for combining multibaseline Pol-InSAR results, Pol-InSAR inversion performances are considerably improved. The eccentricity method (*Figure 5* on the left) tends to slightly overestimate low to medium forest heights (10 m to 30 m), but estimation results for stands taller than 30 m fit very well. The obtained results are fairly good with a correlation coefficient r^2 of 0.92 and a root mean square error (RMSE) of 2.33 m.

The validation plot of the height accuracy method is shown in *Figure 5* on the right. Height accuracy results are better than results obtained by the eccentricity method with a correlation coefficient of 0.93 and a RMSE of 1.97. This method seems to be highly practical for forest height estimation when multibaseline data sets are on hand.

6. CONCLUSIONS

In this paper, multibaseline Pol-InSAR inversion approaches have been proposed and addressed in order to reduce constraints for single baseline Pol-InSAR inversion such as non-volumetric decorrelation effects and the height sensitivity of the vertical wavenumber. Multibaseline Pol-InSAR inversion could contribute to compensate or filter out inversion results with strong height errors. Consequently the combination of multiple Pol-InSAR height estimates can improve significantly forest height inversion accuracy. The best multibaseline height estimate has an r^2 of 0.93 with RMSE of 1.97 m. The overall estimation accuracies for both multibaseline inversion approaches were better than 10% height error.

7. REFERENCES

[1] S.R. Cloude and K.P. Papathanassiou 1998, "Polarimetric SAR Interferometry", IEEE Transactions on Geoscience and Remote Sensing, vol. 36, no. 5, pp. 1551-1565, September 1998.

[2] K.P. Papathanassiou and S.R. Cloude, ‘‘Single-baseline Polarimetric SAR Interferometry’’, IEEE Transactions on Geoscience and Remote Sensing, vol. 39, no. 11, pp. 2352-2363, 2001.

[3] S.R. Cloude and K.P., Papathanassiou, “Three-stage inversion process for polarimetric SAR interferometry”, IEE Proceedings - Radar Sonar and Navigation, vol. 150, no. 3, pp. 125-134, 2003

[4] Hajnsek, F. Kugler, S.-K. Lee, K. P. Papathanassiou, “Tropical-Forest-Parameter Estimation by means of Pol-InSAR: The INDREX II Campaign”, IEEE Transactions on Geoscience and Remote Sensing, vol. 47, no. 2, pp. 481 – 493, February 2009

[5] J. Praks, F. Kugler, K.P. Papathanassiou, I. Hajnsek and M. Hallikainen, “Height estimation of boreal forest: Interferometric model-based inversion at L- and X-band versus HUTSCAT profiling scatterometer”, *IEEE Geosci. Remote Sens. Lett.*, vol. 4, no. 3, pp.446-470, Jul. 2007.

[6] F. Kugler, F.N. Koudogbo, K.P. Papathanassiou and K. Gutjahr, “ Frequency effects in Pol-InSAR forest height estimation”, in *Proc. EUSAR*, Dresden, Germany, May 16-18, 2006.

[7] F. Kugler, S.K. Lee and K.P. Papathanassiou, “Estimation of Forest Vertical Structure Parameter by means of Multi-baseline Pol-InSAR”, *in Proc. IEEE IGARSS*, Cape Town, South Africa, July 2009.

[8] P. A. Rosen, S. Hensley, I. R. Joughin, F. K. Li, S. N. Madsen, E. Rodriguez, and R. M, Goldstein, “Synthetic aperture radar interferometry,” *Proc. IEEE*, vol. 88, no. 3, pp. 333–382, Mar, 2000

[9] I. Hajnsek, K.P. Papathanassiou and S.R. Cloude, “Removal of additive noise in polaimetric eigen value processing”, *in Proc. IEEE IGARSS*, Sydney, Australia, 2001, pp. 2778-2780.

[10] R. Bamler, P. Hartl, “Synthetic aperture radar interferometry”, Inverse Problems, vol.14, no. 4, pp. R1-R54,1998

[11] T. Flynn, M. Tabb and R. Carande, “Coherence region shape extraction for vegetation parameter estimation in polarimetric SAR interferometry”, Proceedings of the IEEE International Geoscience and Remote Sensing Symposium (IGARSS), June, Toronto, Canada, vol. 5, pp.2596-2598 , 2002

[12] R.T. Fomena and S.R. Cloude, “On the Role of Coherence Optimization in Polarimetric SAR Interferometry”, CEOS SAR Cal / Val Workshop, Adelaide, Australia, September 28-30, 2005

[13] S. R. Cloude (2009). *Polarisation*, Oxford University Press, Oxford, UK, pp240-246.

[14] H. A. Zebker and J. Villasenor, “ Decorrelation in interferometric radar echoes”, *IEEE Transactions on Geoscience and Remote Sensing*, vol. 30, no. 9, pp. 950 – 959, January 1992.

[15] R.N. Treuhaft, S.N. Madsen, M. Moghaddam, and J.J. van Zyl, “Vegetation Characteristics and Underlying Topography from Interferometric Data”, Radio Science, vol. 31, pp. 1449-1495, 1996.